CAMBRIDGE
UNIVERSITY PRESS

Research Paper

SN1991bg-like supernovae are associated with old stellar populations

Fiona H. Panther[1,2,3] (ORCID), Ivo R. Seitenzahl[1,2], Ashley J. Ruiter[1,2,3], Roland M. Crocker[2], Chris Lidman[2,3], Ella Xi Wang[2], Brad E. Tucker[2,4,5] and Brent Groves[2,4]

[1]School of Science, UNSW Canberra, Australian Defence Force Academy, Canberra, ACT 2612, Australia, [2]The Research School of Astronomy and Astrophysics, Mount Stromlo Observatory, Australian National University, Canberra, ACT 2611, Australia, [3]ARC Centre of Excellence for All-Sky Astrophysics (CAASTRO), Canberra, Australia, [4]The ARC Centre of Excellence for All-Sky Astrophysics in 3 Dimensions (ASTRO 3D), Canberra, Australia and [5]National Centre for the Public Awareness of Science, Australian National University, Canberra, ACT 2611, Australia

Abstract

SN1991bg-like supernovae are a distinct subclass of thermonuclear Type Ia supernovae (SNe Ia). Their spectral and photometric peculiarities indicate that their progenitors and explosion mechanisms differ from 'normal' SNe Ia. One method of determining information about supernova progenitors we cannot directly observe is to observe the stellar population adjacent to the apparent supernova explosion site to infer the distribution of stellar population ages and metallicities. We obtain integral field observations and analyse the spectra extracted from regions of projected radius $\sim$ kpc about the apparent SN explosion site for 11 91bg-like SNe in both early- and late-type galaxies. We utilise full-spectrum spectral fitting to determine the ages and metallicities of the stellar population within the aperture. We find that the majority of the stellar populations that hosted 91bg-like supernovae have little recent star formation. The ages of the stellar populations suggest that that 91bg-like SN progenitors explode after delay times of >6 Gyr, much longer than the typical delay time of normal SNe Ia, which peaks at $\sim$1 Gyr.

Keywords: galaxies: stellar content – supernovae: general – supernovae: individual: SN1991bg – techniques: imaging spectroscopy

(Received 09 November 2018; revised 03 July 2019; accepted 03 July 2019)

1. Introduction

Type Ia supernovae (SNe Ia) are usually described as a photometrically and spectroscopically homogeneous class of astrophysical transients. They are thought to arise from the thermonuclear disruption of a carbon–oxygen (CO) white dwarf (WD) star in an interacting binary system [see Hillebrandt et al. (2013) and Maguire (2017) for a review]. 'Normal' SNe Ia are standardisable candles (Branch & Tammann 1992): there is a tight relation between their peak luminosity and the width of their light curve (the Phillips 1993 relation), and between their peak luminosity and their optical colour at peak luminosity (Tripp 1998). Thus, they make an excellent tool for measuring cosmological distances. As standardisable candles, normal SNe Ia have been employed in cosmology to probe the geometry of the universe (Riess et al. 1998; Perlmutter et al. 1999; Leibundgut 2001). However, the proliferation of SN surveys over the past 30 yr has led to the discovery of several spectroscopically and photometrically peculiar subclasses of these events. The discovery of SN1991bg in particular (Filippenko et al. 1992)—the prototype event for the SN1991bg-like subclass of SNe Ia [hereafter 91bg-like SNe, see Taubenberger

(2017) for a review]—challenged the accepted paradigm that SNe Ia are a homogeneous class of events.

91bg-like SNe events share several key features with their normal SNe Ia cousins, and are clearly thermonuclear supernovae. Specifically, they lack any indication of hydrogen and helium in their spectra while also exhibiting strong Si II in absorption (Filippenko 1997). Moreover, absorption features in their spectra near maximum light indicate the presence of a number of intermediate mass elements (IMEs) including silicon, magnesium, calcium, sulphur, and oxygen. The presence of these IMEs is consistent with these events belonging to the class of thermonuclear transients (Filippenko 1997). However, 91bg-like SNe also exhibit significant photometric and spectroscopic peculiarities compared to normal SNe Ia. This is highly suggestive of a different explosion mechanism and/or progenitor configuration. This subclass differs from 'normal' SNe Ia in the following ways:

- 91bg-like SNe are subluminous compared to SNe Ia by 1.5–2.5 mag at optical maximum, reaching peak absolute magnitudes of only −16.5 to −17.7 in B (Taubenberger 2017),
- 91bg-like SNe are significantly redder than their normal SNe Ia cousins, with $(B − V)_{max}$ = 0.5–0.6 mag,
- 91bg-like SNe light curves decline very quickly and are characterised by a light curve decline parameter $1.8 \leq \Delta m_{15}(B) \leq 2.1$, compared to $\Delta m_{15}(B) \leq 1.7$ for normal SNe Ia. 91bg-like SNe also have a light curve rise time of $\sim$13–15 d (Taubenberger et al. 2008), a few days shorter than normal SNe Ia. Combined with their low peak luminosities, this is consistent with these events

synthesising significantly lower ^{56}Ni masses than their normal SNe Ia counterparts ($\sim$0.05–0.1 M$_\odot$, Sullivan et al. 2011).

- 91bg-like SNe lack a secondary maximum in the near infrared (NIR), unlike normal SNe Ia, likely due to the 91bg-like SNe ejecta being cooler and less luminous than that of the normal SNe Ia. Instead, they exhibit a single NIR maximum delayed a few days with respect to the maximum in B (Garnavich et al. 2004), whereas the first NIR peak in a normal SN Ia light curve precedes the B band maximim. The absence of the secondary NIR maximum makes it impossible to perform a simple time shift to make the 91bg-like SNe light curve map to the standardisable light curve of the normal Ia, and the absence of the feature is physically interpreted as a merging of the primary and secondary NIR maxima into a single maximum due to the physical conditions in the SN ejecta (Kasen 2006; Blondin, Dessart, & Hillier 2015).

- Spectroscopically, 91bg-like SNe exhibit similar pre-maximum optical spectra to normal SNe Ia—i.e. dominated by IMEs. However a transition to a spectrum dominated by iron group elements happens earlier in 91bg-like SNe than in normal SNe Ia (Taubenberger 2017).

- Particularly notable is the presence of unusually strong Ti II and O I λ7774 in absorption in the post-maximum spectra. A number of these spectral peculiarities can be attributed to the unusually cool and slow-moving ejecta ($\sim$7 000 km s^{-1}, Taubenberger et al. 2008) when 91bg-like SNe are compared to normal SNe Ia: the lower ionisation state favours a higher abundance of neutral and singly ionised species. However, it is considered unlikely that ionisation state and temperature explains all these spectral peculiarities.

To explain the spectroscopic and photometric peculiarities of 91bg-like SNe, a variety of progenitors and explosion mechanisms have been suggested. A 'violent merger' of two near-equal mass CO WDs was explored via hydrodynamical simulations in Pakmor et al. (2010). Although the light curves of the these explosions were somewhat too broad to reproduce observations of 91bg-like SNe, the synthesised spectra, red colour, and low expansion velocities were a fairly good match to observed properties of 91bg-like SNe. To better reproduce the characteristics of 91bg-like SNe light curves, it was suggested by Pakmor et al. (2013) that the faint, fast light curves of 91bg-like SNe could result from the merger of a CO WD and a helium WD (e.g. see their Figure 4). The smaller ejecta mass that is expected in such an explosion can naturally explain the observed narrower light curves of 91bg-like SNe compared to their 'normal', brighter counterparts. A specific formation channel of the same progenitor scenario (CO WD + He WD merger) was found by Crocker et al. (2017) to plausibly supply the high ^{44}Ti yield that is necessary for these merging events to also explain the positron annihilation signal in the Milky Way.

While a number of progenitor configurations and explosion mechanisms have been suggested to explain the properties of 91bg-like SNe, no direct observations of the progenitor systems have been made, and so the exact progenitors of these SNe remain unknown. One method of inferring information about the progenitors of SNe independent of the observed properties of the explosion is to consider the galaxies in which they occur. A qualitative connection between host galaxy properties and the occurrence of 91bg-like SNe has already been well established. In LOSS (the Lick Observatory Supernova Search, Li et al. 2011), around 15% of all SNe Ia were of the 91bg-like SNe subclass. However, considering only early-type galaxies, the fraction of SNe Ia that are of the

91bg-like SNe subtype rises to 30%. Furthermore, in Perets et al. (2010) the cumulative distribution of 91bg-like SNe occurring in galaxies of various Hubble types was found to be different to that of SNe Ia. More recently, the LOSS sample was used to quantify the SNe luminosity–stellar age connection in Shen, Toonen, & Graur (2017) together with binary population synthesis models. In that work, it was shown that double WD systems with less massive primaries result in fainter SNe Ia at long ($>$1 Gyr) delay times, in agreement with the simulations of Pakmor et al. (2010) and the theoretical arguments of Crocker et al. (2017).

SNe Ia are observed to occur in all galaxy types, from passive to star forming, and there is some evidence that they are found in regions of galaxies occupied by older, several Gyr-old stars (e.g. the vertical distribution of SNe Ia is greater than the vertical distribution of Core collapse supernovae (CCSNe) in edge-on spiral galaxies Hakobyan et al. 2017). On the other hand, 91bg-like SNe occur predominantly in early-type galaxies (Perets et al. 2010). While this is clear, a specific connection between the properties of early-type galaxies (which tend to be more massive, more metal-rich, host significantly less star formation, and contain older stellar populations) and 91bg-like SNe is yet to be firmly established.

A number of works (Gallagher et al. 2008; Stanishev et al. 2012; Rigault et al. 2013; Galbany et al. 2014; Rigault et al. 2018) have now investigated the connection between the global properties of galaxies and the observed stretch and colour of SNe Ia, as this may be a source of bias in cosmology. While the focus has been on 'normal' SNe Ia, Gallagher et al. (2008) noted a correlation between older stellar populations and lower luminosity SNe Ia. Several of their low-luminosity supernovae were classified spectroscopically as SNe 91bg in the Berkeley Supernova Project (Silverman et al. 2012), and their host galaxies were found to contain stars with an average age of $\sim$10 Gyr.

The observations of Gallagher et al. (2008) were restricted to early-type galaxies and utilised slit spectroscopy. Consequently, the ages and metallicties of the stellar populations derived represent a single global average for these SNe host galaxies. Since these host galaxies are early-type galaxies where the stellar populations will be well-mixed, the global galaxy properties are a good approximation for the stellar population that gives rise to the supernova progenitor (Galbany et al. 2014). However, the method employed by Gallagher et al. (2008) makes it hard to exclude the presence of recent local star formation within a few kiloparsecs of the supernova progenitor. Furthermore, the Gallagher et al.'s (2008) work makes use of the Lick/IDS Index system (Worthey 1994; Worthey & Ottaviani 1997) to derive the average age and metallicity of the stellar populations of the observed galaxies, and does not take into account that stellar population will be composed of stars that formed at different times and thus cannot be characterised by a single stellar age.

Global galaxy properties may help with the standardisation of supernova light curves; however, to determine whether a supernova subtype is associated with an old ($>$2–3 Gyr old) stellar population requires one to rule out the presence of recent star formation within a few kiloparsecs of the apparent supernova explosion site.

To do this, it is necessary to consider a spectrum of the stellar population adjacent to the apparent supernova explosion site. Integral Field Unit (IFU) observations can be utilised to investigate this. For nearby supernova hosts (up to $z \sim 0.03$), an aperture with a radius of $\sim$1.5 arcsec can resolve a region around 1 kpc in projected radius on the galaxy. Furthermore, a local measurement can also be used to determine the distribution of stellar population

ages using a method such as penalised pixel fitting of the stellar spectrum extracted from the same aperture used in step one (Cappellari & Emsellem 2004; Cappellari 2017).

In this work, we will utilise penalised pixel fitting to investigate the age distribution of the stellar populations that hosted 91bg-like supernovae in a range of galaxies of all morphological types. We choose to use the local stellar spectra at the supernova explosion site as opposed to integrated galaxy spectra. For example, in the case of a late-type host galaxy, star formation may be localised to the disc of a galaxy. In an integrated spectrum of the galaxy, this star formation can dominate the observed light due to the luminosity of O-A stars. Thus, if a supernova occurs in the bulge of a spiral galaxy - dominated by an old stellar population - one is likely to underestimate the age of the population that gave rise to the SN progenitor if only global galaxy properties are considered. On the other hand, if an SN occurs in an early-type galaxy where significant stellar migration may have occurred, one can still use the IFU technique to constrain the age of the supernova progenitor: if an SN progenitor is formed within the last Gyr, evidence of this star formation will still be apparent in the stellar spectra as stars will not migrate far from their birthplaces in this time frame (Fujii & Baba 2012). Furthermore, the local stellar population will have a distribution of ages representative of that of the whole galaxy (Galbany et al. 2014).

Several works have utilised a similar method, employing IFU spectroscopy to investigate the region in the immediate projected vicinity of SNe Ia to determine the relationship between the scatter in SNe Ia properties after standardisation, and star formation rate (Stanishev et al. 2012; Rigault et al. 2013, 2018). Those works are particularly important in the context of cosmology, as the dispersion in Hubble residuals can affect the precision and accuracy of measurement of the cosmological parameters, such as the Hubble constant and the dark energy equation of state parameter. However, the properties of stellar populations at the explosion sites of different subtypes of SNe Ia have not yet been studied in detail. 91bg-like SNe are a distinct subclass which are empirically shown to occur predominantly in old stellar populations. Thus, they provide a perfect opportunity to use IFU spectroscopy to quantify the age of stellar populations close to the SN explosion site and constrain the presence of recent star formation.

In this paper, we present the results of our observations of 91bg-like SNe host galaxies using IFU spectroscopy based on data obtained at Siding Spring Observatory (SSO). We derive the distribution of stellar population ages and metallicities of the stars in a region of radius $\sim$1 kpc around the apparent SN explosion site using full-spectrum fitting. Our observations and data reduction are described in Section 2, and the results of the full-spectrum fitting procedure is described in Section 3. Finally, we present a discussion of our results in Section 4 and our conclusions in Section 5.

2. Observations and data reduction

2.1. Sample selection

Our sample of 91bg-like SNe host galaxies is composed of 15 hosts of SNe spectroscopically identified as 91bg-like SNe by Silverman et al. (2012) visible from SSO, as well as the host of SN2012fx (Pastorello et al. 2012) and the host of lsq15bb (Fremling et al. 2015). We do not make any selection cuts based on galaxy morphology, luminosity, or mass. Nor do we make a selection cut against supernovae that have large offsets from their host as there

may be a diffuse stellar population present at the explosion site not obvious in the Digitized Sky Survey 2 (DSS-2[a]) images which were used to create finder charts for each observation.

2.2. Observations

We obtained integral field observations of 17 spectroscopically identified 91bg-like SNe host stellar populations using the WiFeS instrument (Dopita et al. 2007) on the Australian National University 2.3 m Advanced Technology Telescope at SSO.

Observations were obtained over a total of 14 nights between July 2016 and February 2017. WiFeS is a wide-field IFU with a total field of view of 25 arcsec $\times$ 38 arcsec. The instrument configuration is shown in Table 2. The aperture of WiFeS is centred on the apparent location of each SN, with the position angle of the aperture chosen to minimise contamination from nearby stars but, as we only extract spectra from pixels close to the apparent SN location, the position angle has little practical importance.

Exposure times reflect changes in our observation strategy to account for inclement weather conditions. A summary of all our science observations is given in Table 1. Bias frames, Cu–Ar arcs, and dome flats were obtained at the beginning and end of the night. Wire frames[b] were obtained at the end of each night, and sky flats were obtained at the beginning of each night. For each individual galaxy observation, Cu–Ar arcs (required for accurate wavelength solution, which may drift a few angstroms over the course of a night) and bias frames are obtained within 30 min of the observation, and each galaxy observation is accompanied by at least one sky frame, which is used to remove skyline contamination. Finally, a spectrophotometric standard star is observed on each night of observation. Where weather conditions did not permit time for these observations, spectrophotometric calibration was carried out using a spectrophotometric standard taken in earlier runs, with the standard frames being taken in similar photometric weather conditions and at similar air mass to the galaxy being observed.

2.3. Data reduction

Data reduction was facilitated by the `PyWiFeS` data reduction package (Childress et al. 2014a). The pipeline produces a spectrophotometrically calibrated and fully coadded data cube, and a corresponding parallel-processed error cube. At this point, a number of SN hosts are removed from the sample due to the observations having either been undertaken in inclement weather (see footnote c in Table 1), or of an SN explosion site with a large offset from the SN host galaxy; thus, the signal to noise ratio (SNR) in the data cube is inadequate to obtain either a local or global stellar spectrum associated with the SN host.

Spectra of the stellar populations local to each SN were then extracted from the calibrated data cube. We use a seeing-limited aperture of 3 arcsec $\times$ 3 arcsec centred on the apparent location of the SN in each host galaxy (the physical size of these apertures varies with redshift and is shown in Table 1). These spectra are processed to remove residual sky lines using a nearby area free from galaxy light, offset from the host galaxy from the same final data cube, and the mean resulting spectrum is extracted from the 3 arcsec $\times$ 3 arcsec region of interest.

Each remainingspectrum is then shifted to rest-frame wavelength according to the host redshift listed on NASA Extragalactic

---

[a]http://archive.eso.org/dss/dss.
[b]A wire frame ensures the spectrograph slits are appropriately aligned on the CCD.

Table 1. Summary of observations.

SN Name	Host galaxy	SN RA	SN DEC	t_{exp} (s)	Morph[a]	A_{ap} (kpc^2)	z
SN1993aa	Anon J230322-0620	23 03 22.02	−06 20 56.1	$2 \times 1\,800$	10	1.23	0.018
SN2000ej	IC1371	21 20 15.66	−04 52 40.5	$2 \times 1\,800$	−5	3.6	0.0308
SN2007ba	UGC9798	15 16 41.83	+07 23 48.1	$2 \times 1\,800$	0	5.5	0.03825
SN2007cf	MCG+02-39-021	15 23 07.66	+08 31 45.5	$2 \times 1\,800$	−2	4.1	0.03293
SN2007fq	MCG-04-48-19	20 34 55.92	−23 06 15.84	$2 \times 1\,800$	−2	6.8	0.04245
SN2012fx[b]	ESO417-03	02 55 41.20	−27 25 27.59	$4 \times 1\,800$	5	1.2	0.0176
SN2002cf	NGC4786	12 54 31.30	−06 51 24.8	$3 \times 1\,200$	−5	0.9	0.015
SN2002jm	IC603	10 19 25.20	−05 39 14.5	$2 \times 1\,200$	1	1.3	0.0182
SN2007al	Anon J095919-1928	09 59 18.48	−19 28 25.8	$3 \times 1\,200$	−5	0.6	0.0121
SN2008ca	SDSS J122901.28-263305.6	12 29 01.20	+12 22 18.84	$3 \times 1\,200$	10	55	0.123
SN2008bt	NGC3404	10 50 16.99	−12 06 31.5	$3 \times 1\,200$s	1	0.91	0.0154
SN2002ey[c]	Anon J23101188+0732541	23 10 12.33	+07 32 59.9	$2 \times 1\,800$	−1	5.7	0.0388
SN2005er[c]	NGC7385	22 50 00.84	+11 37 05.7	$3 \times 1\,800$	−2	2.6	0.02616
SN2005ke[c]	NGC1317	03 35 04.35	−24 56 38.8	$3 \times 1\,200$	0	0.2	0.00643
SN2007N[c]	MCG-01-33-12	12 49 01.25	−09 27 10.2	$3 \times 1\,200$	1	0.6	0.0126
SN2006gt[c]	Anon J005618-0137	00 56 17.30	−01 37 46.0	$3 \times 1\,800$	−5	7.5	0.0447
lsq15bb[c,d]	2dFGRS TGN352Z120	09 58 51.95	+01 01 04.12	$3 \times 1\,200$	0	23	0.08

[a] Morphology based on DSS R-band images classified by the authors using numerical Hubble types where negative numbers represent early-type galaxies, and positive numbers late-type (de Vaucouleurs 1959).
[b] SN classification from Pastorello et al. (2012).
[c] Removed from sample due to low SNR in data cube due to adverse weather conditions or SN at large offset from host.
[d] SN classification from Fremling et al. (2015).

Table 2. WiFeS instrument configuration.

Component	Configuration
Red grating	R3000
Blue grating	B3000
Dichroic	RT560
Wavelength range	∼3 300–9 200 Å

Database (NED),[c] which is checked against the redshift we derive from either the narrow Hα line if present, or the H and K lines for the remaining galaxies. The spectra are then corrected for Milky Way dust reddening using `brutus 0.3.1`.[d] Galactic extinction is derived using NED from the Schlafly & Finkbeiner (2011) recalibration of Schlegel, Finkbeiner, & Davis (1998) infrared-based dust map. The map is based on dust emission from Cosmic Background Explorer (COBE)/Diffuse Infrared Background Experiment (DIRBE) and Infrared Astronomical Satellite (IRAS)/Infrared Sky Survey Atlas (ISSA); the recalibration assumes a Fitzpatrick (1999) reddening law with $Rv = 3.1$ and different source spectrum than Schlegel et al. (1998). The resulting spectra are subsequently ready for analysis.

3. Results

3.1. Full spectrum fitting

Deriving stellar population ages requires simultaneous determination of both the age of stars and their metallicity as there is a

significant degeneracy between the effect of metallicity and age on galaxy spectra (Worthey 1994).

We use the publicly available penalised pixel fitting code (pPXF, Cappellari & Emsellem 2004; Cappellari 2017) to fit linear combinations of simple stellar populations (SSPs) from the MILES stellar library (Sánchez-Blázquez et al. 2006; Vazdekis et al. 2010), which provides 985 stellar spectra across a wavelength range of 3 525–7 500 Å at 2.5 Å spectral resolution, for stellar metallicities ranging from $[M/H] = 0.22$ to $[M/H] = -2.3$. The 'solution' of the problem—to fit multiple SSPs to an observed spectrum—is defined by different weights applied to each SSP in a regular grid in log-age and metallicity space. The program outputs a weighted average age of the stellar population and a weighted average metallicity according to these weights, along with information about the weights applied to each age-metallicity bin. This allows us to determine both the distribution of stellar population ages that contribute to the spectrum, and the weighted average age of the stellar population, as well as whether any substantially younger or older stellar population than the average is present.

We obtain a fit to the total spectrum of 11 91bg-like SN host galaxies (with flux normalised by the flux at 5 500 Å). pPXF decomposes the spectra into nebular and stellar components, and determines the mass fraction of stars into age and metallicity bins determined by the available grid of SSP models.

In Figure 1, we show outputs from pPXF which display the mass fraction of stars in age and metallicity bins. The majority of stellar populations we observe exhibit similar characteristics to Figure 1(b), including the local stellar population of SN2012fx, which occurred in the bulge of a late-type galaxy. These stellar populations have a large mass fraction of stars at ages ∼10 Gyr at super-solar metallicities ($[M/H] > 0$). The weighted average stellar population properties of seven of our observed SN explosion
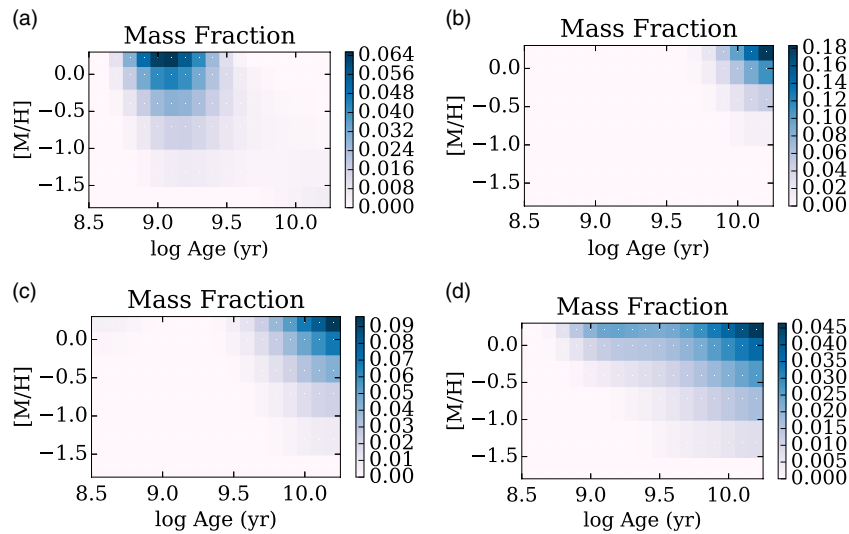
Figure 1. Mass fraction of stars in different age and metallicity bins based on spectra extracted from 3 arcsec × 3 arcsec regions centred on the SN explosion site in each galaxy, which are interpreted as representing the distribution of stellar population ages which give rise to the SN progenitor. The radius of the aperture in physical units is shown in each subcaption. The population shown in (b) is representative of the remaining seven galaxies for which the stellar populations are fitted with pPXF. (a) Stellar pop. within 0.57 kpc of SN1993aa. (b) Stellar pop. within 0.96 kpc of SN2000ej. (c) Stellar pop. within 0.49 kpc of SN2008bt. (d) Stellar pop. within 3.44 kpc of SN2008ca.

sites suggest that 91bg-like SNe occur preferentially in stellar populations with ages ∼10 Gyr with solar, or slightly sub-solar metallicities (Figure 3) (Table 3).

Three of the observed stellar populations, however, contain a younger stellar component: the host of SN1993aa [Figure 1(a)], the host of SN2008bt [Figure 1(c)], and the host of SN2008ca [Figure 1(d)]. The spectra of these galaxies are also unusual in comparison to the majority of the galaxies observed. An example of a typical spectrum we analyse with pPXF is shown in Figure 2(a). This spectrum corresponds to the population shown in Figure 1(b), and is composed predominantly of old, metal-rich stars. In comparison, the spectrum of the host population of SN1993aa [Figure 2(b)] is significantly bluer and exhibits strong emission lines of Hα, [N II], [S II], [O III], and Hβ. The strong emission lines indicate there may be ongoing star formation in this stellar population, in good agreement with the high mass fraction of stars with ages ∼1 Gyr seen in Figure 1(a). Similarly, the host population of SN2008ca also exhibits strong emission lines [Figure 2(d)]; however, the spectrum is (within the noise) somewhat less bluer than that of SN1993aa, suggesting an older stellar component may also be present [Figure 1(d)]. While the physical area of the aperture within the host of SN1993aa encompasses ∼1 kpc, it should be noted that the host of SN2008ca is significantly more distant than that of SN1993aa and therefore the entire galaxy, with an area of ∼50 kpc is sampled in the aperture. This may be the reason we observe apparent multiple stellar populations in this SN host galaxy. An example of a more resolved galaxy that also exhibits multiple stellar populations is the host of SN2008bt. This galaxy has strong Hα, [N II] and [S II] emission [Figure 2(c)], and while it has a predominantly old stellar population, there is a small mass fraction of stars which have an age of ∼0.5 Gyr [Figure 1(c)]. When we consider the position of the aperture on the host galaxy, we see that while the SN has occurred in a position that may be coincident with the bulge of the galaxy, because the galaxy is viewed almost edge on, there may be some contamination of starlight and nebular emission from a younger, star-forming disc. While we cannot rule out that the supernova occurred in this region, we do find that the majority of the stellar

mass within the aperture is concentrated in the old, metal-rich stellar population.

3.2. Comparison sample of SNe Ia

While we wish to quantify the ages and metallicities of the stellar populations that host 91bg-like SNe, we also wish to compare the distribution of stellar population ages and metallicities to a sample of SNe Ia host galaxies to investigate whether 91bg-like SNe differ in some way. Unfortunately, a representative sample of SNe Ia host galaxies with spectra of the stellar population in the immediate vicinity of the apparent SN location is not publicly available. However, in Maoz, Mannucci, & Brandt (2012) a sample of Sloan Digital Sky Survey (SDSS) galaxies that hosted SNe Ia is compiled. As a comparison sample, we compute the weighted average stellar population age and metallicity for these galaxies using pPXF. We note that this average is for the integrated light of the host galaxy where the SDSS fibre is centred on the core of the galaxy, and not solely the stellar population ∼1 kpc from the apparent supernova location; however, it has been previously noted that the global properties of SNe Ia host galaxies correlate well with the properties local to the SN explosion site (Galbany et al. 2014).

We find that the weighted average ages of stellar populations have a wide, almost uniform distribution, with ages between ∼30 Myr and >10 Gyr. The metallicity distribution is peaked towards super-solar metallicities ([M/H] > 0). We also find that the older the stellar population of the galaxy, the more metal-poor the weighted average metallicity becomes.

3.3. Stellar populations hosting SNe 91bg

As a further comparison, we overplot the stellar population ages and metallicities determined using slit spectroscopy for early type galaxies hosting SNe 91bg from Gallagher et al. (2008). The black markers in Figure 3 show the ages and metallicities of these galaxies. These ages and metallicities are determined using Lick indicies (Worthey 1994; Worthey & Ottaviani 1997) which rely
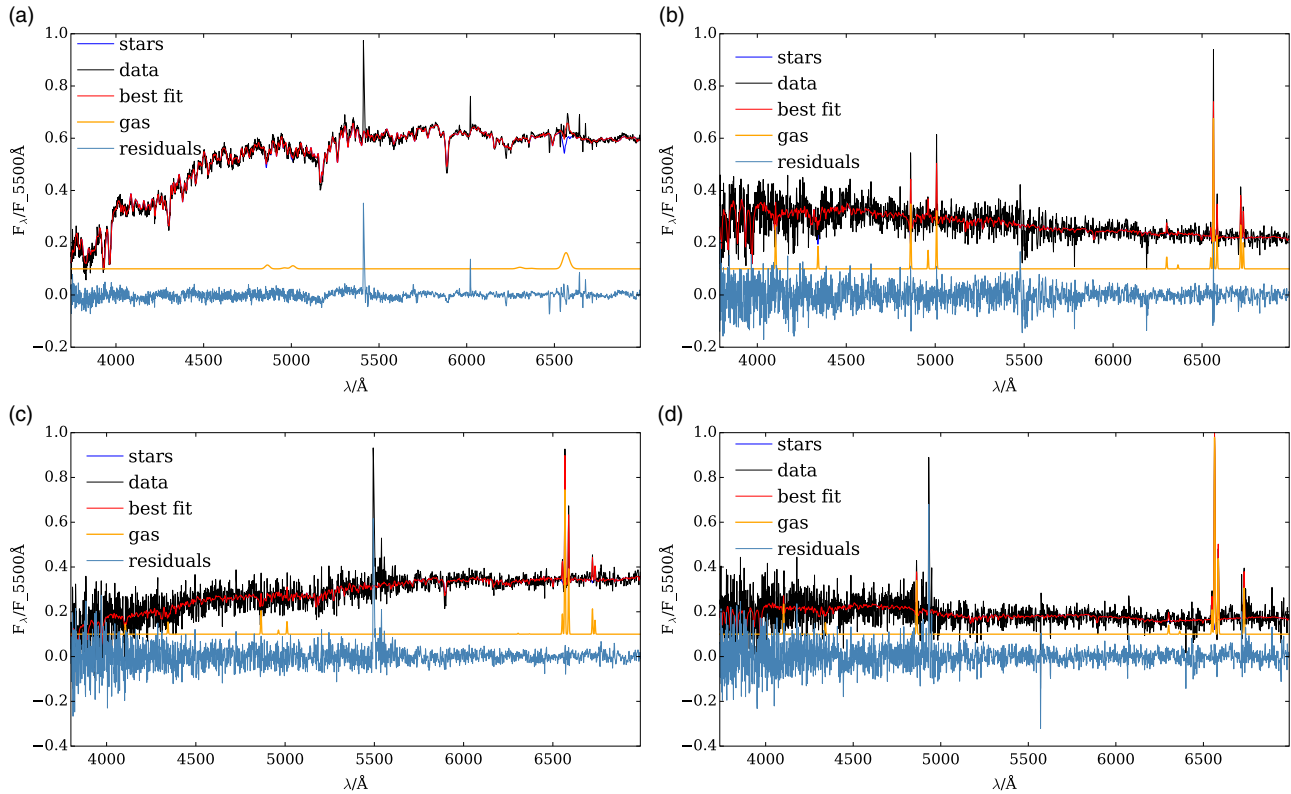
Figure 2. Spectra fitted using pPXF. Data are shown in grey, and the best fit to the total spectrum (nebular plus stars) in red. The spectrum is also decomposed into stellar (dark blue) and nebular spectra (orange). Residuals for the best fit are shown in light blue. For several of the spectra, there are substantially larger residuals towards bluer wavelengths due to the lower SNR at blue wavelengths. (a) Fitted spectrum of SN2000ej host. (b) Fitted spectrum of SN1993aa host. (c) Fitted spectrum of SN2008bt host. (d) Fitted spectrum of SN2008ca host.

Table 3. Summary of results.

SN name	Host galaxy	$<\log(\text{age/yr})>$	$<[M/H]>$
SN1993aa	Anon J230322-0620	$9.173^{+0.047}_{-0.193}$	$-0.19^{+0.21}_{-0.31}$
SN2000ej	IC1371	$10.08^{+0.05}_{-0.19}$	$0.03^{+0.05}_{-0.25}$
SN2007ba	UGC9798	$10.04^{+0.06}_{-0.11}$	$-0.01^{+0.09}_{-0.27}$
SN2007cf	MCG+02-39-021	$10.05^{+0.05}_{-0.11}$	$0.00^{+0.07}_{-0.26}$
SN2007fq	MCG-04-48-19	$10.08^{+0.04}_{-0.09}$	$0.04^{+0.04}_{-0.23}$
SN2012fx[2]	ESO417-03	$9.993^{+0.08}_{-0.11}$	$-0.03^{+0.09}_{-0.27}$
SN2002cf	NGC4786	$10.04^{+0.06}_{-0.11}$	$-0.16^{+0.19}_{-0.32}$
SN2002jm	IC603	$10.05^{+0.05}_{-0.10}$	$0.01^{+0.07}_{-0.26}$
SN2007al	Anon J095919-1928	$10.03^{+0.07}_{-0.10}$	$-0.16^{+0.18}_{-0.31}$
SN2008ca	SDSS J122901.28-263305.6	$9.685^{+0.255}_{-0.185}$	$-0.13^{+0.18}_{-0.17}$
SN2008bt	NGC3404	$9.939^{+0.11}_{-0.07}$	$-0.08^{+0.14}_{-0.28}$

on comparing the measured equivalent width of different absorption lines found in galaxy spectra to an irregular diagnostic grid computed from SSPs. As these galaxies were observed using slit spectroscopy, the stellar populations are representative of the average age of the stars contained in the whole galaxy. Compared to the SNe Ia comparison sample taken from Maoz et al. (2012), the galaxies that host SNe 91bg in Gallagher et al. (2008) appear to contain older stellar populations. Furthermore, the ages and metallicities derived for these galaxies are consistent with the ages and metallicities of the local stellar populations of SNe 91bg we derive from our observations.

4. Discussion

In this work, we analysed the spectra of galaxies observed with the WiFeS IFU. This allowed us to isolate the stellar population within a few kiloparsecs of the apparent SN explosion site, and determine the age and metallicity of the stellar population in the vicinity of the SN. The age of the stellar population surrounding the SN explosion site in particular may constrain the delay time distribution of 91bg-like SNe (the distribution of times between the SN progenitor formation and the subsequent SN explosion).
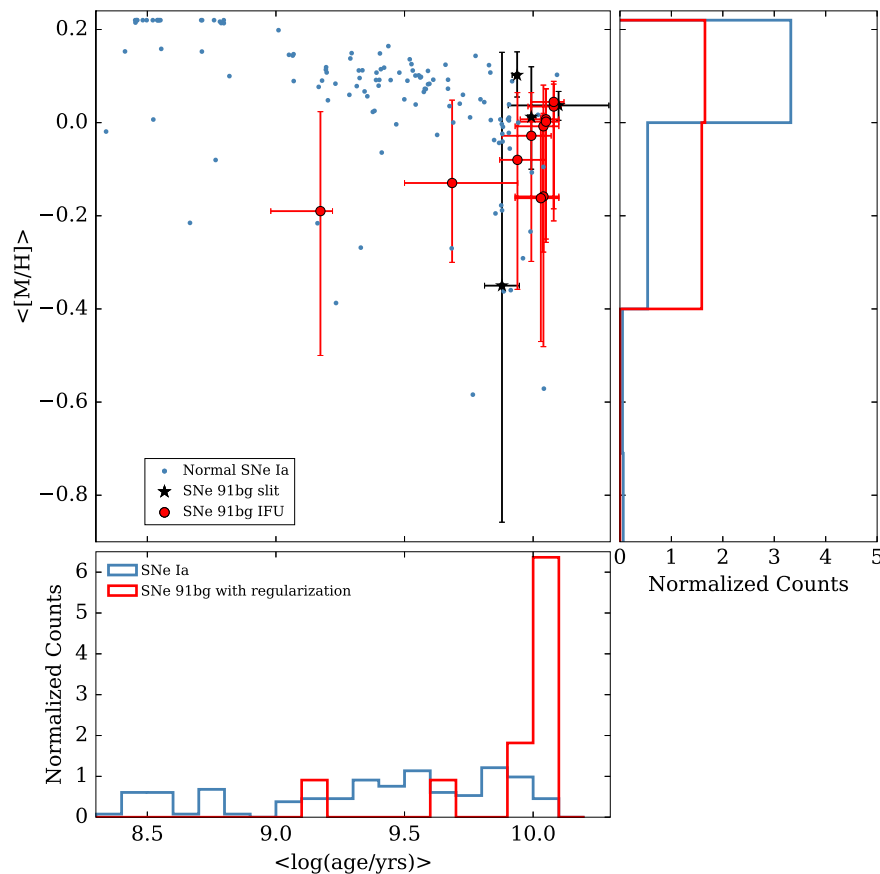
Figure 3. Weighted average stellar population ages for SDSS spectra of galaxies that hosted SNe Ia, based on the sample presented in Maoz et al. (2012) (blue) and for the local stellar populations of SNe 91bg galaxies (red). Error bars show the 16th and 84th percentile of the distribution of stellar population ages and metallicities based on the Cumulative distribution function (CDF) of stellar population properties. Black points show the ages and metallicities of SNe 91bg host galaxies observed in Gallagher et al. (2008), derived using Lick/IDS indicies and their respective errors. The histograms show the distribution of weighted average stellar population ages (bottom) and metallicities (right). The binning reflects the available metallicities and ages of the stellar population templates in the MILES library used to fit the spectra.

In particular, we find that the stellar populations that host SNe 91bg have greater weighted average stellar population ages than those of SNe Ia and many lack evidence of recent star formation. This is strong evidence that 91bg-like SNe are not associated with recent star formation (within the last ~1 Gyr), as the stellar spectra lack evidence of a significant number of O-A stars being present. Furthermore, these results suggest that the delay time distribution of 91bg-like SNe is peaked towards very long delay times (10 Gyr), in contrast with SNe Ia, whose delay times peak at ~1 Gyr (Childress et al. 2014b). We compared our derived average stellar population ages and metallicities for the local stellar populations of SNe 91bg with the stellar population ages and metallicities of SNe 91bg host galaxies found by Gallagher et al. (2008) and find a good agreement within the error bars between the two results.

We note, however, the large errors on the metallicity of the stellar populations in both our own measurements and those from Gallagher et al. (2008). While two different methods are used to determine the stellar population parameters—full spectrum fitting with pPXF in this work and the Lick/IDS index system in Gallagher et al. (2008)—the stellar model library used to compute stellar population ages and metallicities is identical (the MILES library, Vazdekis et al. 2010). While these stellar templates are well sampled in the age parameter space, there are only seven available metallicities between $[M/H] = -2.3$ and $[M/H] = 0.2$. Although

the metallicity computed by full spectrum fitting is accurate, it lacks the precision that would be possible with a finer grid of models in metallicity space. This is reflected by the error bars shown in Figure 3.

The SNe 91bg host galaxies from Gallagher et al. (2008) are part of a larger sample of massive elliptical galaxies that hosted thermonuclear supernovae. As massive elliptical galaxies typically contain older stellar populations, there is likely a bias towards sampling host stellar populations where we expect the relative rate of SNe 91bg to normal SNe Ia to be somewhat higher than average. In our sample, we make no selection cuts and select galaxies of any morphological classification that hosted SNe 91bg. The majority of the host galaxies we observe are selected from the Berkeley Supernova Project (BSNIP) sample (Silverman et al. 2012). These supernovae were observed as part of a targeted, local survey. Consequently, the galaxies in which SNe in a targeted survey occur tend to be more massive, and SNe that occur in less massive galaxies may be missed. As a result, there may be some bias towards sampling older stellar populations, since more massive galaxies tend to contain older, more metal-rich stars. However, we have also observed SNe 91bg hosts that were not targeted by BSNIP and in which 91bg-like SN occurred more recently, in particular the host of SN2012fx, a nearby spiral galaxy for which the apparent SN explosion site is in the galactic bulge. The stellar population local

to the SN explosion site is found to be relatively typical of those found in the BSNIP sample and has a weighted average stellar population age of ~10 Gyr.

We also compare our stellar population average ages and metallicities with those derived for the host galaxies of SNe Ia as observed by SDSS, based on a sample from Maoz et al. (2012). There may be some bias associated with our measurement of stellar population ages for these SNe Ia host galaxies as the SDSS fibre is placed over the centre of the galaxies they observe. This means that one is likely to observe most of the integrated light from the central, bulge regions of these galaxies, biasing our results to older ages as the star-forming, younger outer regions of some galaxies observed by SDSS are missed by the fibre. Consequently, the weighted average plotted in Figure 3 may not represent the exact properties of the stellar population close to the explosion site and therefore may represent an upper limit on the stellar population age.

We find that SNe Ia are hosted by galaxies that exhibit a broad range of weighted average stellar population ages, from the very young at 30 Myr to the very old (~10 Gyr). This is in contrast to the stellar populations that host SNe 91bg, which cluster at the substantially older end of this distribution. This demonstrates that SNe 91bg may be associated with progenitors that tend to occur at longer delay times than SNe Ia [e.g. as suggested in Crocker et al. (2017)]. We find that while around half of our observed galaxies have Hα emission and nebular emission indicating recent star-formation activity, the majority of galaxies are dominated by absorption lines and have no strong emission lines. Moreover, with the exception of the host of SN1993aa, the regions of the galaxies that hosted 91bg-like SNe that exhibit emission lines are also found to contain older (~10 Gyr) stellar populations.

Note that while we find that 91bg-like SNe are associated with older populations than SNe Ia, this result does not preclude that the same galaxy could host both types of supernovae. Indeed, two examples of galaxies hosting both supernovae are SN1991bg and SN1957B (an SN Ia), which both occurred in M84, and of the 91bg-like supernova SN2006mr in Fornax A (Maoz & Mannucci 2008), which also hosted five SNe Ia. The point here is that while the delay time distribution of SNe Ia may peak at 1 Gyr (Childress et al. 2014*b*), SNe Ia can still occur in stellar populations with much greater ages (see Figure 1). Moreover, both M84 and Fornax A are early-type galaxies and will likely be dominated (in terms of number) by an old stellar population from which the 91bg-like supernova progenitors may arise but they may also contain younger populations that could host SNe Ia progenitors. It is important to note that while we find that 91bg-like SNe are associated with older populations than SNe Ia, our results are not contradicted by these observations. Our comparison sample of SNe Ia from Maoz et al. (2012) shows evidence that while the delay time distribution of SNe Ia may peak at 1 Gyr (Childress et al. 2014*b*), SNe Ia can still occur in stellar populations with much greater ages (see Figure 3). Thus it is possible for SNe Ia and 91bg-like supernovae to occur in the same host galaxy even if the delay time distribution of the progenitors is quite different.

We note that the MILES stellar population models we used with pPXF assume the evolution of single stellar populations only. While tracking the stellar evolution and corresponding spectral morphology of single stars is relatively straightforward, it is fairly complicated in the case of interacting stars. Though the majority of stars in the Universe are likely part of a binary (or

higher order) star system (Moe & Di Stefano 2017), most spectral synthesis codes ignore the effects that binary (and multiple) stellar evolution have on the integrated light from galaxies due to the added layer of complexity (e.g. mass transfer and variation from single star evolutionary pathways) that must be taken into account. However, recent work has shown that incorporating binary star evolution models into spectral synthesis analysis codes does indeed result in different derived physical properties (Stanway, Eldridge & Becker 2016). On the other hand, the difference between single star spectral synthesis codes, such as GALEXEV, and binary spectral synthesis programs, like Binary Population and Spectral Synthesis (BPASS), is more prominent at early times, in particular for stellar ages ≲1 Gyr [see Stanway & Eldridge (2018), Figure 2, right column]. Since the explosion sites that we are probing mostly consist of relatively old stellar populations, we are thus not overly concerned that our derived stellar properties are very different from the properties we would expect those stellar populations to have. A comparison of derived stellar properties with a spectral synthesis program that incorporates binaries (such as BPASS) is beyond the scope of this work, though based on the work of Stanway & Eldridge (2018), we would plausibly expect our derived stellar ages to decrease slightly, while the derived metallicities may slightly increase.

5. Summary and conclusions

We obtained integral field observations of the apparent explosion sites of 17 91bg-like SNe; 11 of these observations yielded spectra of sufficiently high signal-to-noise ratio to derive information about the stellar population within ~1 kpc projected radius of the explosion site. Using full-spectrum fitting, we found that the majority of the stellar populations that host 91bg-like SNe we observe are dominated by old, metal-rich stars. The majority lack evidence of recent star formation. We conclude that the SNe 91bg progenitors are unlikely to be associated with recent star formation, and likely have delay times >6 Gyr. This favours a progenitor model such as that proposed in Pakmor et al. (2013) or Crocker et al. (2017), which is composed of a He WD and CO WD.

References

Blondin, S., Dessart, L., & Hillier, D. J. 2015, MNRAS, 448, 2766
Branch, D., & Tammann, G. A. 1992, ARA&A, 30, 359
Cappellari, M. 2017, MNRAS, 466, 798
Cappellari, M., & Emsellem, E. 2004, PASP, 116, 138
Childress, M. J., Vogt, F. P. A., Nielsen, J., & Sharp, R. G. 2014a, Ap&SS, 349, 617
Childress, M. J., Wolf, C., & Zahid, H. J. 2014b, MNRAS, 445, 1898
Crocker, R. M., et al. 2017, NA, 1, 0135 EP
de Vaucouleurs, G. 1959, Handbuch der Physik, 53, 275
Dopita, M., Hart, J., McGregor, P., Oates, P., Bloxham, G., & Jones, D. 2007, Ap&SS, 310, 255
Filippenko, A. V. 1997, ARA&A, 35, 309
Filippenko, A. V. et al. 1992, AJ, 104, 1543
Fitzpatrick, E. L. 1999, PASP, 111, 63
Fremling, C., et al. 2015, The Astronomer's Telegram, 6909
Fujii, M. S., & Baba, J. 2012, MNRAS, 427, L16
Galbany, L., et al. 2014, A&A, 572, A38
Gallagher, J. S., Garnavich, P. M., Caldwell, N., Kirshner, R. P., Jha, S. W., Li, W., Ganeshalingam, M., & Filippenko, A. V. 2008, ApJ, 685, 752
Garnavich, P. M., et al. 2004, ApJ, 613, 1120
Hakobyan, A. A., et al. 2017, MNRAS, 471, 1390
Hillebrandt, W., Kromer, M., Röpke, F. K., & Ruiter, A. J. 2013, FP, 8, 116
Kasen, D. 2006, ApJ, 649, 939
Leibundgut, B. 2001, ARA&A, 39, 67
Li, W., et al. 2011, MNRAS, 412, 1441
Maguire, K. 2017, in Handbook of Supernovae (Springer) 293, doi:10.1007/978-3-319-21846-5_36
Maoz, D., & Mannucci, F. 2008, MNRAS, 388, 421

Maoz, D., Mannucci, F., & Brandt, T. D. 2012, MNRAS, 426, 3282
Moe, M., & Di Stefano, R. 2017, ApJS, 230, 15
Pakmor, R., Kromer, M., Röpke, F. K., Sim, S. A., Ruiter, A. J., & Hillebrandt, W. 2010, Nature, 463, 61
Pakmor, R., Kromer, M., Taubenberger, S., & Springel, V. 2013, ApJ, 770, L8
Pastorello, A., et al. 2012, The Astronomer's Telegram, 4339
Perets, H. B., et al. 2010, Nature, 465, 322
Perlmutter, S., et al. 1999, ApJ, 517, 565
Phillips, M. M. 1993, ApJ, 413, L105
Riess, A. G., et al. 1998, AJ, 116, 1009
Rigault, M., et al. 2013, A&A, 560, A66
Rigault, M., et al. 2018, preprint arXiv:1806.03849
Sánchez-Blázquez, P., et al. 2006, MNRAS, 371, 703
Schlafly, E. F., & Finkbeiner, D. P. 2011, ApJ, 737, 103
Schlegel, D. J., Finkbeiner, D. P., & Davis, M. 1998, ApJ, 500, 525
Shen, K. J., Toonen, S., & Graur, O. 2017, ApJ, 851, L50
Silverman, J. M., et al. 2012, MNRAS, 425, 1789
Stanishev, V., Rodrigues, M., Mourão, A., & Flores, H. 2012, A&A, 545, A58
Stanway, E. R., & Eldridge, J. J. 2018, MNRAS, 479, 75
Stanway, E. R., Eldridge, J. J., & Becker, G. D. 2016, MNRAS, 456, 485
Sullivan, M., et al. 2011, ApJ, 732, 118
Taubenberger, S. 2017, in Handbook of Supernovae (Springer), 317, doi:10.1007/978-3-319-21846-5_37
Taubenberger, S., et al. 2008, MNRAS, 385, 75
Tripp, R. 1998, A&A, 331, 815
Vazdekis, A., Sánchez-Blázquez, P., Falcón-Barroso, J., Cenarro, A. J., Beasley, M. A., Cardiel, N., Gorgas, J., & Peletier, R. F. 2010, MNRAS, 404, 1639
Worthey, G. 1994, ApJS, 95, 107
Worthey, G., & Ottaviani, D. L. 1997, ApJS, 111, 377